Energy loss from a moving vortex in superfluid helium

R. J. Zieve, C. M. Frei, and D. L. Wolfson

Energy Loss from a Moving Vortex in Superfluid Helium

R.J. Zieve, C.M. Frei, and D.L. Wolfson

Physics Department, University of California at Davis

We present measurements on both energy loss and pinning for a vortex terminating on the curved surface of a cylindrical container. We vary surface roughness, cell diameter, fluid velocity, and temperature. Although energy loss and pinning both arise from interactions between the vortex and the surface, their dependences on the experimental parameters differ, suggesting that different mechanisms govern the two effects. We propose that the energy loss stems from reconnections with a mesh of microscopic vortices that covers the cell wall, while pinning is dominated by other influences such as the local fluid velocity.

I. INTRODUCTION

The entropy of a superfluid flow is entirely contained in its excitations, the most striking of which are the quantized vortex lines. A question in many situations is how energy transfer and dissipation occur within a superfluid. Energy can shift from one length scale to another, or between the fluid and macroscopic objects such as the container or an object moving through the fluid. Energy can also be dissipated as phonons or other excitations within the fluid.

Much of the recent work on energy transfer has centered on superfluid turbulence, where experiments indicate that different mechanisms act in various temperature regimes. At high temperatures, the superfluid coexists with a normal fluid. Turbulence in the latter has the standard behavior of classical turbulence, and through a coupling between the two components the superfluid takes on the classical behavior as well [1–3]. Yet the same power-law behavior of vortex line density as a function of time, albeit with an altered prefactor, also applies at lower temperature, where only a negligible amount of normal fluid remains and its coupling to the superfluid is drastically reduced [4]. Only when the method of injecting energy into the flow changes does the functional form itself change [5, 6]. On the other hand, while the velocity field in classical turbulence follows a Gaussian distribution with only minor deviations appearing three standard deviations from the peak [7], recent measurements of superfluid turbulence find non-Gaussian behavior with a $1/v^3$ form beginning about one standard deviation from the peak [8]. The degree to which superfluid turbulence mimics classical behavior remains an open question.

Vortex reconnections play a major role in superfluid turbulence. When two vortices closely approach each other, they form cusps that are drawn further together at the tips. Eventually the connectivity at the tips of the cusps changes; effectively each cusp is divided in half and one side of a cusp connects to half of what was originally the other cusp. Similar behavior occurs when a vortex closely approaches a wall of a container. A cusp again appears which splits in two, and each portion terminates on the wall. The cusps created in the reconnection process induce Kelvin waves along the vortices. The Kelvin waves can transfer energy to smaller length scales or radiate energy as sound [9, 10], and in some cases the increased motion may lead to further reconnections [11]. Reconnections in superfluid helium have only recently been visualized [12] and are also difficult to simulate since they in-

volve small length scales and large velocities [13, 14]. Hence different types of observations of reconnections are useful for better understanding the phenomenon. Here we describe how reconnections may affect the energy loss from a single moving vortex.

Our apparatus consists of a straight wire, stretched parallel to the axis of a cylindrical tube [15]. The wire can serve as the core of a superfluid vortex. Alternatively, a vortex can use the wire as its core from one end of the cylinder to somewhere in the middle, then leave the wire and continue to the side wall of the cylinder as a free vortex. The wire's vibration frequencies, which we monitor with an electromagnetic technique, are sensitive to the exact spot where the vortex detaches from the wire. We can observe various aspects of the motion of the free portion of the vortex through effects on the detachment point. For example, in this geometry the free vortex precesses around the wire, driven by the flow field of the trapped circulation. The displacement of the wire from the axis of the cylinder forces the length of the free vortex to change during the precession, which leads to oscillations of the detachment point that conserve the total energy stored in the vortex [16].

From our previous studies of vortex precession, the energy loss rate is many orders of magnitude larger than expected from bulk mutual friction as the vortex moves through the superfluid [17]. A natural assumption is that the dissipation instead originates from the contact between the vortex and the wall of the container. An additional observation confirms the presence of a significant vortex-wall interaction: occasionally a precessing vortex pins on the wall, producing a characteristic signature that includes oscillations with higher frequency and smaller amplitude than those associated with precession, accompanied by an abrupt cessation of the energy loss [18]. Computer simulations, using the assumption that the wall end of the vortex suddenly stops moving, reproduce all these features. Very plausibly, forces strong enough to interrupt the vortex motion completely could also in a less extreme situation induce energy loss. Here we present further experimental results on the interaction of a vortex line with the wall. Our new measurements suggest that different mechanisms produce the pinning and the dissipation, with reconnections responsible for the latter.

II. EXPERIMENTAL SETUP

Our cylindrical cell is mounted vertically on a pumped ^{3}He cryostat. We fill the cell with ^{4}He through a small inlet hole in one end. A fine wire is stretched vertically through the cell. We apply a constant horizontal magnetic field, typically of order 25 mT. To make our measurements, we pass a brief current pulse through the wire. Because of the static magnetic field, the current creates a force displacing the wire from its equilibrium position. After the pulse ends, the wire vibrates under the influence of its own tension, eventually settling back to its equilibrium position. During the vibration, the motion through the horizontal magnetic field induces an emf across the ends of the wire. This is the signal we monitor. In our studies we create vortices by rotating the cryostat at low temperatures, but we make all our measurements with the cryostat stationary.

Vorticity trapped around all or part of the wire alters the observed vibration frequencies. We focus particularly on the frequency splitting between the two lowest modes. The earliest measurements with a straight vibrating wire [19] confirmed the quantization of circulation in superfluid helium, since the frequency splitting expected from a single quantum of circulation was strikingly stable. However, intermediate values of the splitting are also seen. We do not take these as evidence of a non-quantum vortex trapped along the entire wire; rather, they indicate that a quantized vortex covers only a fraction of the wire and hence has a reduced effect on its vibration frequencies. The clean and reproducible signatures we find in several situations [15, 18] confirm this interpretation. As noted above, we can use the frequency splitting of the vibrational modes as an instantaneous measurement of the length of wire covered by the vortex.

For the present measurements we designed new cells that allow us to explore the influence of smoothness more thoroughly and also to probe the effect of cell radius on the vortex-wall interaction. Our previous work showed [15] that the wire mounting can significantly affect the precession behavior. For example, the dissipation is especially high when the wire is far off-center. We also know that for a given wire the energy loss depends on the amplitude of the wire's motion, so other details of the wire's vibration are likely to play a role as well. In particular the vibration frequency varies significantly among wires, from 124 Hz to 791 Hz for the wires discussed here. The dissipation rates that we observe for various wire suggest that other mounting factors which we have not identified also come into play. To enable direct comparison between wall treatments, we make cells that change inner diameter halfway along their length, as shown in Figure 1.

Using a single wire and comparing behavior between the two halves of the same cell eliminates any dependence on the wire's location, its normal modes, the magnetic field needed to excite the vibration properly, and the excitation pulse's shape and amplitude. These latter factors determine the initial motion of the wire, which subsequently moves under the influence of the trapped circulation. As noted above, the wire's motion itself affects the energy loss from the moving vortex; hence keeping the wire velocity constant through a set of mea-

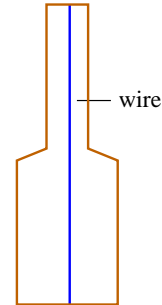surements is important for meaningful interpretation.

FIG. 1: Schematic of typical cell, with diameter changing near the center.

We identify which half of the cell the vortex is in from the precession period. The flow field around the wire drives the precession, and a cell of larger radius includes fluid that is more distant from the wire and hence not moving as fast. This reduces the average speed of the flow, so the free vortex moves more slowly around the cell. In fact the precession period depends on the square of the local diameter, which produces a significant change when the vortex moves from one portion of the cell to the other.

With these cells we can observe directly how cell diameter influences dissipation. We can also investigate the effect of wall roughness, since the diameter change makes polishing only one half of the cell straightforward. We do the polishing mechanically, inserting a Q-tip with diamond powder by hand while rotating the cylinder in a drill press chuck. We use down to 3 micron diamond powder, resulting in surface roughness of less than 50 nm. We test roughness by cutting open polished cells longitudinally and using a surface roughness comparator. The measured 50 nm finish agrees with typical polishing results on other materials, where ultimate surface roughness is typically one or two orders of magnitude smaller than the abrasive grain size [20–22].

III. KELVIN WAVES

In our previous work [18], we found several factors that influence the energy loss from the precessing vortex. Dissipation increases with increasing temperature, longer time between measurements, and lower excitation of the wire during measurements. All of these effects seem to have a common source, an influence of the wire's vibration on the dissipation: the faster the wire moves, the slower the rate of energy loss from the vortex. We hypothesized that the wire influences the dissipation by inducing Kelvin oscillations along the portion of the vortex stretching between the wire and the cell wall. Here we confirm that the wire does indeed excite Kelvin waves along the vortex.

In our new cells, vortices regularly pin at the lip in the middle of each cell where the inner diameter changes. Once pinned, dislodging a vortex is extremely difficult. Unlike other wall pins, where vortices often come free unassisted or
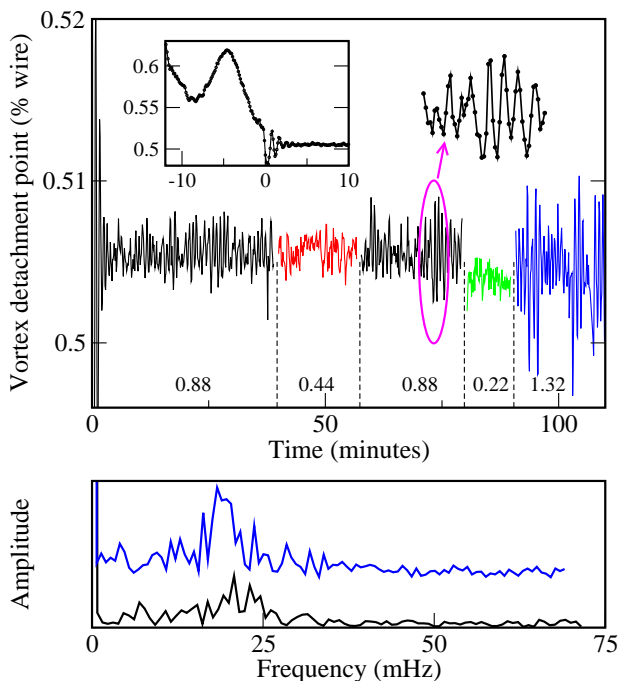
FIG. 2: (Color online) (a) Attachment point position of pinned vortex, for several vibration amplitudes. The numbers near the bottom give the maximum displacement at the center of the wire, in microns, for each data segment. Left inset: precession of vortex before it pins. Right inset: expanded view of the fluctuations in the attachment point location, showing a characteristic frequency. (b) Magnitude of the Fourier transform of the attachment position, for 0.88 μm wire excitation (lower curve, black online) and 1.32 μm wire excitation (upper curve, blue online). The curves are shifted from each other vertically for clarity.

after vibrating the wire with larger amplitude than usual, the lip pins rarely work themselves free. Depinning requires comparable perturbation, either mechanical or thermal, to depinning from the end of the container for a vortex that runs along the wire for the entire length of the cell. The stability of the pin lets us monitor how varying the wire's vibration amplitude affects the pinned vortex.

Figure 2a tracks a pinned vortex as we vary the excitation amplitude of the wire. The maximum displacements at the center of the wire are noted. The variation in the measured attachment position *increases* for larger vibration amplitudes. This is exactly opposite from the expected behavior of our measurement error, since a higher wire excitation typically improves the signal-to-noise as we identify the wire's vibration frequencies. One exception is when the wire is so distorted from its ideal shape that higher-frequency modes become significant as well as the low-frequency oscillations we analyze; another is if the oscillations from one measurement do not die away completely before the wire is excited again. By examining the traces resulting from individual excitations of the wire, we have verified that neither of these potential problems is an issue here. Indeed, as expected, the error in the curve fitting we do to extract the vibration frequencies goes down as the wire excitation increases.

A more careful examination of the fluctuations about the pin level shows that they are not random noise, but have a characteristic oscillation period of about 45 seconds. The expanded picture of the right inset clearly shows several measured points per period. Figure 2b presents Fourier transforms of the attachment position for the two largest wire excitations, which produce maximum displacements of 0.88 and 1.32 μm. Both have peaks near 22 mHz, the frequency corresponding to 45 seconds, with a stronger peak for the larger excitation. Thus the increased variation about the pin level is actual motion of the vortex line rather than noise, and the most natural possibility is the lowest Kelvin mode. Since the vortex is pinned at the cell wall but free to move along the wire, we calculate the period of the Kelvin oscillation with quarter-wavelength equal to the cell radius. For a wave on an infinite straight vortex, the period is approximately

$$T = \frac{2\lambda^2}{\kappa \ln(\lambda/2\pi a)},$$

where $\kappa = 9.97 \times 10^{-4}$ is the circulation quantum, $a = 1.3 \times 10^{-8}$ cm is the core radius of a free vortex, and λ is the wavelength of the Kelvin oscillation. These data are from wire D$'$, with small-side radius 0.16 cm, which yields an ideal Kelvin wave period of 52 s, fairly close to the observed value of 45 s. The larger-amplitude oscillations immediately after the pin starts do have period 52 s. The period may be reduced to 45 s for subsequent Kelvin waves if the vortex pin site shifts slightly into the transition region between the two cell diameters, where the radius is larger. The amplitude increase with wire oscillation amplitude and the agreement with the expected Kelvin wave period show that the wire itself does excite Kelvin waves along the free portion of the vortex.

IV. DISSIPATION

We next present data on the energy loss during precession in cells with one half polished. In Figure 3a, the two halves of the cell have radius 1.6 mm and 2.9 mm, with the larger end polished. Precession begins in the wider half of the cell, with a period of 485 seconds. At the halfway point, the detached portion of the vortex enters the narrower part of the cell and the precession period shifts abruptly to 252 seconds, reflecting the faster average velocity field in this region. The downward slope of the precession trace indicates the steady decrease in length of the trapped vorticity, which corresponds to a significant energy loss. The trapped vortex stores energy per length $\frac{\rho\kappa^2}{4\pi} \ln \frac{R}{r_w}$, where $\rho \approx 0.145$ g/cm^3 is the superfluid density, $\kappa = 9.97 \times 10^{-4}$ cm^2/s is the quantum of circulation, R is the cell radius, and $r_w \approx 8.7 \mu$m is the radius of the wire. For this cell, the energy per length of a trapped vortex is 6.66×10^{-8} erg/cm at the larger radius and 5.98×10^{-8} erg/cm on the smaller side. Initially the slope is 0.14% per minute on the large-diameter side. For our 5 cm long wire this converts to 7.8×10^{-12} erg/s. In the thin half of the cell, the much steeper slope corresponds to energy loss of 47×10^{-12} erg/s.

Previous experimental [15] and computational [23] work has found that changes in energy loss and precession period

are related, with an increase in dissipation corresponding to a longer period. However, that relationship holds for precession within a cell of fixed diameter, not for the change in precession period with cell diameter that we observe here. The present relationship between precession period and dissipation actually goes in the opposite direction: the faster energy loss occurs when the period is longer. Thus the previously known correspondence between dissipation and precession period does not explain our present observations.
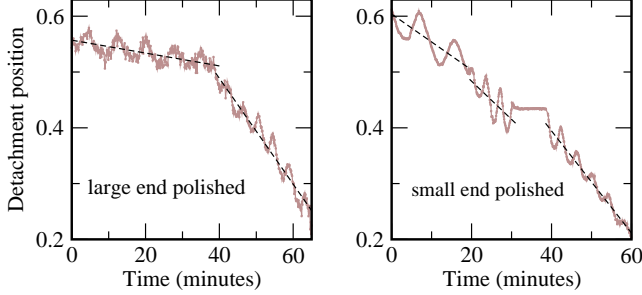

FIG. 3: Vortex precession, moving from the large-diameter end to the small-diameter end, in two cells. The dashed black lines are fits indicating the slope of the different precession segments.

Figure 3b is less dramatic. This cell also has diameters 1.6 mm and 2.9 mm, but with the narrow end polished. Again the vortex begins in the wider half, and again the change in precession period near the attachment position of 0.5 indicates its entry into the smaller part of the cell. Here too there is a change in the dissipation rate, although it is a much smaller shift from 28×10^{-12} erg/s to 37×10^{-12} erg/s. After about 2.5 periods on the narrow end, the vortex pins to the cell wall, depinning by itself after a few minutes. The dissipation rate increases to 46×10^{-12} erg/s after the pin.

The precession periods and energy loss rates of Figure 3 are typical for these two cells. Figure 4 is a compendium of results from all the observed precession events. Figure 4a shows data from the cell of Figure 3a with the wide end polished, while Figure 4c has the narrow end polished. The decay rates are plotted as a function of precession period. They segregate cleanly into narrow-end precession, with period less than 5 minutes, and wide-end precession, with period more than 7 minutes. No precession periods lie in the intermediate region. For both cells, the dissipation is less in the wide portion. In addition, for a given diameter the dissipation is less on average in the cell with that side polished. For the cell of Figure 3a the influence of diameter and smoothness act in the same direction, and the smooth wide side has dramatically less dissipation than the rough narrow side. On the other hand, the cell of Figure 3b shows much less distinction between its rough wide side and smooth narrow side.

To test that other features of the wire mounting, such as the wire's cross-section, its exact location within the cell, or the angle at which the wire enters the stycast cap, are not dominating our observations, we dismantled and remade each of the two cells from the same brass cylinders. All the stycast pieces, as well as the wires, were remade. We did not do any further polishing to the brass cell bodies before reassembling
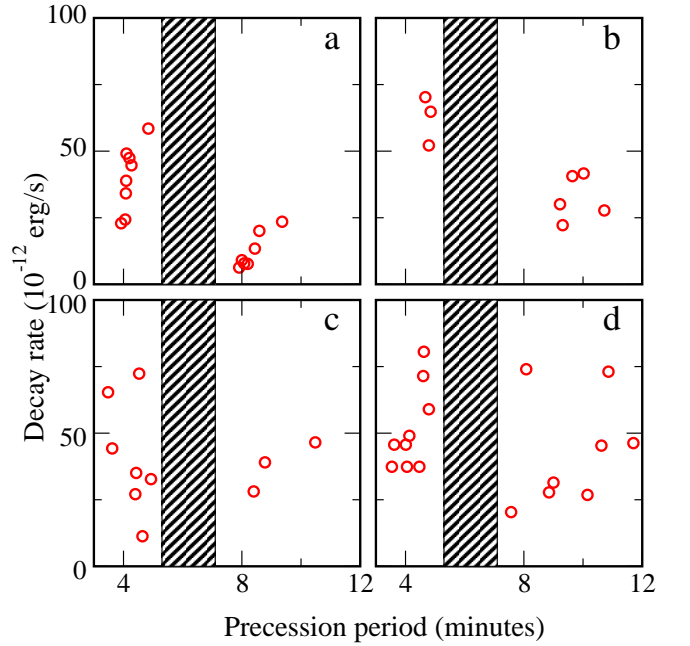

FIG. 4: (Color online) Energy loss rates as function of precession period. Shaded regions show the gap in the precession periods that divides the small-end and large-end motion. Original (a) and remade (b) cell with only large end polished; original (c) and remade (d) cell with only small end polished.

the cells. The precession and decay rate results for the remade cells are shown in Figure 4b and 4d, with the latter including the data from Figure 3b. They show the same trends as for the original cells. The effect of the polishing is less pronounced in the remade cells, possibly because of accumulations on the surfaces over time.

Two additional cells with a diameter change in the middle, G and H in Table I, also exhibit more dissipation on the narrow side. These cells have both ends polished, and the contrast between the two ends is less strong than in cell D but stronger than in cell C. This supports the interpretation that both cell diameter and wall smoothness affect the energy loss.

One known effect of cell diameter is that fluid velocity at the surface decreases with increasing diameter, a result of the $1/r$ velocity dependence of the circulation trapped around the wire. While a lower velocity could plausibly lead to reduced dissipation, one of our measurements suggests that this is not the case. We occasionally see vortex precession in the regime where one quantum of circulation is completely trapped along the wire and a second quantum partly covers the wire. The result is precession at a circulation value between $N = 1$ and $N = 2$, with the vortex driven by a flow field roughly three times as fast as for circulation between $N = 1$ and $N = 0$. The driving field comes from the trapped vorticity, which in the latter case can be approximated as a half-infinite vortex. For circulation between $N = 1$ and $N = 2$, the equivalent approximation uses three half-infinite vortices: two running in one direction from where the vortex detaches and the third running in the other direction. This factor of three has experimental confirmation in the much shorter precession periods

when $N > 1$. However, the energy loss per time during precession for $N > 1$ is comparable to that for $N < 1$. Hence the fluid velocity must not be a key factor in the energy loss.

V. PINNING

We next turn to how smoothness and diameter affect pinning. Table I compiles pinning statistics for several wires. Cells A and B have only a single radius along the entire length; the remainder have a change in diameter as described above. Since the radius of cells A and B is typical of the smaller end of the other cells, we treat all results from those cells as being in the smaller-diameter region. Cells C′ and D′ are the remakes of cells C and D, and the decays pictured in Figure 3 come from wires C and D′. We examine the vortex motion during decays that include a pinning event. As long as there is a sufficiently clear stretch of precession, we can determine from its period which half of the cell contains the pin site. For example, Figure 5 shows a pin surrounded by precession oscillations of period about 11 minutes. The long period indicates that the vortex is on the large-diameter portion of the cell. We assume that any pin close to the center of the cell is at the lip. In some cases the precession is too noisy or too brief to identify where the vortex is. This is mainly an issue with cell E, which was completely unpolished and had very frequent pins.

The pinning properties of the cells described here do not exhibit a correspondence between increased pinning and higher energy loss. More pinning occurs in the larger-diameter portions of cells, despite the fact that the energy loss is lower in these regions. Note that the absolute number of pins is not the correct quantity to compare across cells; the amount of time used to acquire data in each case is relevant, as is the duration of smooth precession atop which pin events can be identified. The final sections of Table I list the total precession time for each half of each cell and normalize the pinning events to the precession time. We also list the precession temperatures in the final column, since the likelihood of pinning does increase with temperature.

We find large variation in the pinning characteristics from one cell to another with nominally similar properties. As far as roughness, which increases the energy loss rate, there is generally more pinning in rougher cells. In an extreme example, the vortex pinned so frequently in the unpolished cell E that no precession ever continued for more than one and one-half circuits of the cell. The only two cells showing more pinning on their polished ends than on their unpolished ends were the two remade cells, C′ and D′. We speculate that accumulations of dust on the walls between the original assembly of these cells and the reassembly might have a larger effect on the polished surfaces. It is possible that dust is a larger factor for these two cells, since before the second assembly we cleaned them only with liquid, in an attempt to avoid adding any additional scratches to the surfaces.

Another indication of the propensity to pin comes from the temperature required for reliably pinning a vortex. In previous work [18], we found that a vortex quickly pins at temper-
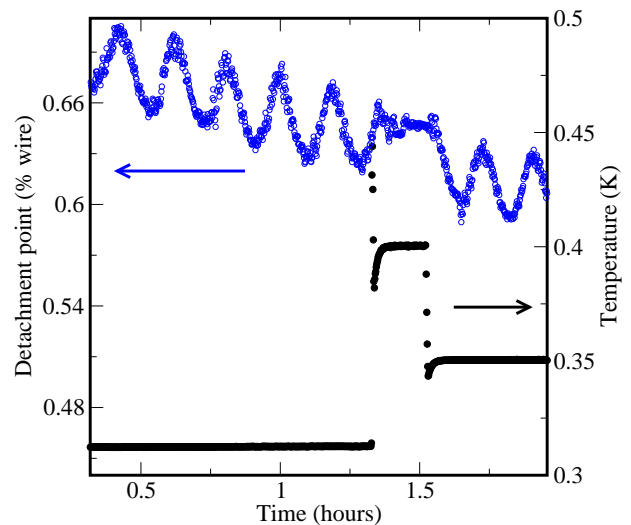

FIG. 5: (Color online) Precession oscillations and pin (blue online, left axis) and cryostat temperature (black online, right axis). The pin occurs just after the temperature is raised from 312 mK to 400 mK, and the vortex depins shortly after the temperature is lowered to 350 mK. Data are from wire G.

atures above 1 K, coming free if and when the temperature again drops below 500 mK. Figure 5 shows a similar effect on wire G, albeit at lower temperature. An increase in temperature from 312 mK to 400 mK triggers the pinning, and the vortex frees itself once the temperature is lowered to 350 mK. Because the signal-to-noise in our measurements is much higher in this temperature range than it is above 1 K, we can see clearly that the precession oscillations cease at 400 mK. The role of elevated temperature in instigating pinning seems qualitatively the same, but the pinning regime now begins at lower temperatures. We conclude that pinning is easier in the new cell. Indeed, we reduced the temperature from 400 mK to 350 mK for many of our precession measurements, since at 400 mK there was so much pinning that we rarely observed significant stretches of precession.

These results expose a difficulty with the idea that Kelvin waves control dissipation through their interaction with the wall roughness. If energy loss is caused by near-pins that the vortex breaks free from, then energy loss and pinning should track each other; if low dissipation indicates few near-pinning events, then one would expect correspondingly few actual vortex pins. Previous observations supported the relationship [18]. For example, increasing temperature leads both to higher dissipation and to a much higher probability of pinning. However, the correspondence does not extend throughut the present work. We summarize our results on both pinning and energy loss in Table II. Notably a larger cell diameter reduces dissipation but increases pinning, while polishing the cell walls reduces dissipation but has a less straightforward effect on pinning. In both cases the change in dissipation is much more reproducible than the effect on pinning. These observations suggest that the two phenomena, while both involving interaction between the precessing vortex and the cell wall, do not in fact stem from the same mechanism.

TABLE I: Summary of wires measured.

cell	radius (mm)	polished	number of pin events				precession time (min)		minutes of precession per pin		
			wide end	narrow end	middle	unknown	wide end	narrow end	wide end	narrow end	temperature
A	1.6	yes	–	2	–	–	–	219	–	110	all below 350 mK
B	1.6	yes	–	0	–	–	–	193	–	>193	300-400 mK
C	1.6, 2.9	1.6	2	0	5	0	465	255	232	>255	350-500 mK
C$'$	1.6, 2.9	1.6	3	7	2	0	225	143	75	20	400 mK
D	1.6, 2.9	2.9	0	0	1	1	430	221	>430	221	375-400 mK
D$'$	1.6, 2.9	2.9	3	1	7	0	262	168	87	168	400 mK
E	1.6, 2.9	no	2	0	0	18	38	35	19	>34	mostly 400mK
F	1.8, 1.9	both	0	0	1	0	–	509	–	>509	400 mK
G	1.8, 3.2	both	9	3	26	0	1366	620	152	207	350 and 400 mK
H	1.8, 3.0	both	0	1	13	3	482	414	>482	414	mostly 400 mK

TABLE II: Influences on pinning and energy loss.

External change	Effect on energy loss	Effect on pinning
smoother cell walls	decreases	usually less
larger cell diameter	decreases	usually more
higher fluid velocity	none	less
more wire vibration (lower T or stronger excitation)	decreases	decreases

VI.   MESH

We suggest a new mechanism for the energy loss during vortex precession, an interaction with a vortex mesh that covers the cell walls. Such a mesh, consisting of short vortex lengths pinned on both ends to the cell wall, is believed to form easily and quickly on container walls, thanks to the extremely small vortex core size in superfluid helium [24]. As the vortex moves along the wall, its end constantly sweeps through the mesh, reconnecting with mesh vortices as it goes. We have confirmed the possibility of energy loss through reconnection in computer simulations [11]. Reconnections lead to Kelvin waves along the vortex line. These waves bring portions of the vortex very close to the wall, leading to vortex-wall reconnections that shorten the precessing vortex line. At the low temperatures of our experiment, the Kelvin waves experience so little damping that many vortex-wall reconnections can result from a single reconnection with a mesh vortex.

This mechanism is qualitatively consistent with several of our observations about the energy loss during precession. Smoother cell walls support a less dense vortex mesh, leading to fewer reconnections and less energy loss. A larger cell diameter should also reduce the vortex mesh, since pinned vortices are less stable near a flatter surface [25]. The mesh mechanism is also compatible with the similar dissipation rates observed for precession between $N = 2$ and $N = 1$ and for precession between $N = 1$ and $N = 0$. Although the additional trapped circulation increases the horizontal speed of the moving vortex, our simulations suggest that the distance along the wall traveled by the end of the vortex is determined mainly by vertical oscillations rather than horizontal motion [11]. Hence the total distance traveled, and therefore the rate of encountering mesh vortices, has little dependence on the fluid velocity in the cell.

A final point is how the wire's vibration interacts with the precessing vortex. As shown in [18], the wire can impart energy to the vortex line, and increasing the average wire velocity reduces the observed energy loss from the vortex. The average wire velocity can be increased by increasing the initial vibration amplitude, by reducing the time between excitations, or by cooling the helium to increase the time constant of the vibration's decay. All methods have the same effect on the moving vortex. One intriguing observation is that the wire excitation never causes the trapped vortex to gain energy, even though the energy lost from the wire in each pulse is much larger than that stored in the partially trapped circulation. As shown in Figure 6, the dissipation rate decreases as the wire motion increases, but it appears to level out at zero. This is consistent with a mesh mechanism of dissipation. Perturbing the vortex more strongly must ultimately lead to a steady-state situation where the energy imparted to the vortex equals the energy removed through reconnections. Stronger perturbations of the vortex lead to a longer steady-state length and increased rate of reconnections.

Interactions with vortices pinned to a surface may be important to other situations, such as energy loss in superfluid turbulence [26] and vortex nucleation [27]. Possible pinning of vortex half-loops to vibrating wires [28] or grids [29] may also be crucial to the interpretation of experimental results, if vortices attached to the probes alter the observed behavior.

One interesting comparison is between the energy loss found in our measurements and in superfluid turbulence. For decaying superfluid turbulence in ^{4}He at low temperatures, the energy loss per time per length of moving vortex is $(0.003)\kappa^3 L\rho$, where L is the line length density [3]. With $L = 18$ cm^{-2}, the dissipation becomes 8×10^{-12} erg/s cm. This value of L corresponds to vortex separation of roughly $L^{-1/2} = 0.24$ cm. Since this is comparable to the length
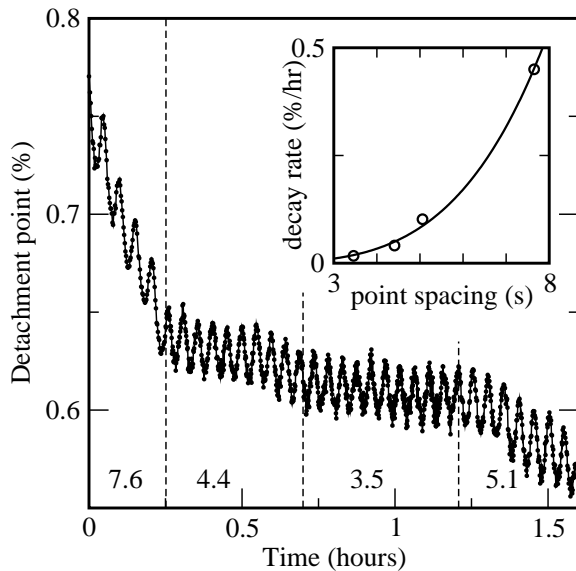
FIG. 6: Influence of wire excitation on vortex energy loss. The intervals between successive excitations range from 3.5 to 7.6 seconds. Energy loss decreases with more frequent excitation, but as shown in the inset it remains positive; strong excitation of the wire does not increase the energy stored in the vortex.

scale in our cells, we expect the vortex velocities to be similar in the two cases. Our observed energy loss is about an order of magnitude larger: 20 to 250×10^{-12} erg/s cm in the large-diameter regions and 70 to 530×10^{-12} erg/s cm for the small-diameter portions. In the experiments on decay of turbulence, scaling behavior which persists to $L = 18$ cm^{-2} indicates a cascade mechanism of transfering energy to ever-smaller length scales. The energy transfer functions through vortex reconnections [30]. If reconnections also govern dissipation in our experiment, through the interaction with wall vortices, then the similarity of the energy loss rates in the two experiments may be more than mere coincidence.

In our wall mesh scenario described above, the pinning comes about for completely different reasons from the energy loss. The energy loss depends on the interaction with a mesh of wall vortices, but there is no obvious reason that the wall vortices should dominate pinning. A more likely influence is the superfluid velocity near a potential pin site, which can sweep a vortex away and prevent pinning. Indeed, we see this experimentally for precession between $N = 2$ and $N = 1$. As noted above, the fluid velocity near the moving vortex is roughly three times as large as in the more common situation where the vortex precession is between $N = 1$ and $N = 0$. Significantly, we have *never* observed pinning at $N > 1$, de-

spite more than seven hours of precession in various wires and more than 35 additional hours with $N > 1$. Pinning also increases in our larger-diameter cells, where the $1/r$ falloff of the field from the trapped vortex yields a much smaller fluid velocity near the cell wall. By contrast, the energy loss depends little on the amount of trapped circulation and decreases with larger cell diameter.

Wall roughness may influence pinning both by providing more irregularities that can serve as pin sites and also by distorting the local velocity field. For rough walls, the fluid has a smaller laminar flow region, and the resulting increase in local flow velocity could reduce vortex pinning. If the stability of a vortex at a pin site depends both on the strength of the pin (e.g., the size and shape of a bump on the wall) and on the details of the nearby fluid flow that might dislodge the vortex, then the dependence of pinning on roughness could be irregular, as observed. Rougher walls would increase both the fluid speed and the typical bump size, but the balance between them might not have any simple behavior.

Our final probe is the wire vibration itself. We reliably observe an increase in pinning with increased temperature. Pinning also seems to increase when we decrease the vibration amplitude for the measurements, although our experiments with changing the amplitude are not extensive. We conclude that wire vibration can dislodge vortices from pin sites.

VII. CONCLUSION

We measure energy loss and pinning for a vortex extending from a vibrating wire in the middle of a cylindrical container to the edge of the container. Both effects stem from interaction between the vortex and the surface, but their different dependence on external parameters, particularly fluid velocity and cell diameter, shows that different mechanisms must be responsible for the two. We propose that energy loss arises from reconnections with a mesh of vortices pinned to the cell wall, which induce further reconnections with the cell wall itself and deposit segments of the moving vortex on the wall. Pinning is instead governed by competition between the degree of roughness on the cell wall and the fluid velocity field near the wall.

VIII. ACKNOWLEDGEMENTS

[1] M. Abid, M.E. Brachet, J. Maurer, C. Nore, and P. Tabeling, *Euro. J. Mech. B, Fluids* **17**, 665 (1998); J. Maurer and P. Tabeling, *Europhys. Lett.* **43**, 29 (1998).

[2] M.R. Smith, R.J. Donnelly, N. Goldenfeld, and W.F. Vinen, *Phys. Rev. Lett.* **71**, 2583 (1993).

[3] P.M. Walmsley, A.I. Golov, H.E. Hall, A.A. Levchenko, and W.F. Vinen, *Phys. Rev. Lett.* **99**, 265302 (2007).

[4] S.I. Davis, P.C. Hendry, and P.V.E. McClintock, *Physica B* **280**, 43 (2000).

[5] P.M. Walmsley and A.I. Golov, *Phys. Rev. Lett.* **100**, 245301

(2008).

[6] M. Tsubota, T. Araki, and S.K. Nemirovskii, *Phys. Rev. B* **62**, 11751 (2000).

[7] A. Noullez, G. Wallace, W. Lempert, R.B. Miles, and U. Frisch, *J. Fluid Mech.* **339**, 287 (1997).

[8] M.S. Paoletti, Michael E. Fisher, K.R. Sreenivasan, and D.P. Lathrop, *Phys. Rev. Lett.* **101**, 154501 (2008).

[9] W.F. Vinen, *Phys. Rev. B* **64**, 134520 (2001).

[10] D. Charalambous, P.C. Hendry, M. Holmes, G.G. Ihas, P.V.E. McClintock, and L. Skrbek, *J. Low Temp. Phys.* **145**, 107 (2006).

[11] I.H. Neumann and R.J. Zieve, *Phys. Rev. B* **81**, 174515 (2010).

[12] G.P. Bewley, M.S. Paoletti, K.R. Sreenivasan, and D.P. Lathrop, *Proc. Nat. Acad. Sci.* **105**, 13707 (2008).

[13] J. Koplik and H. Levine, *Phys. Rev. Lett.* **71**, 1375 (1993).

[14] R. Tebbs, A.J. Youd, and C.F. Barenghi, *J. Low Temp. Phys.* **162**, 314 (2011).

[15] L. Hough, L.A.K. Donev, and R.J. Zieve, *Phys. Rev. B* **65**, 024511 (2001).

[16] R.J. Zieve, Yu.M. Mukharsky, J.D. Close, J.C. Davis, and R.E. Packard, *Phys. Rev. Lett.* **68**, 1327 (1992).

[17] G.W. Rayfield and F. Reif, *Phys. Rev.* **136**, A1194 (1964).

[18] L.A.K. Donev, L. Hough, and R.J. Zieve, *Phys. Rev. B* **64**, 180512 (2001).

[19] W. F. Vinen, *Proc. Roy. Soc. A* **260**, 218 (1961).

[20] H.Y. Tam, H.B. Cheng, and Y.W. Wang, *J. Materials Processing Technology* **192-193**, p. 276-280 (2007).

[21] V.D. Heydemann, W.J. Everson, R.D. Gamble, D.W. Snyder, and M. Skowronski, *Materials Science Forum* **457-460**, p. 805-808 (2004).

[22] Xueping Xu, R.P. Vaudo and G.R. Brandes, *Optical Materials*, **23**, p. 1-5 (03).

[23] K.W. Schwarz, *Phys. Rev.* **B47**, 12030 (1993).

[24] D.D. Awschalom and K.W. Schwarz, *Phys. Rev. Lett.* **52**, 49 (1984).

[25] R.J. Zieve and L.A.K. Donev, *J. Low Temp. Phys.* **121**, 199 (2000).

[26] S.K. Nemirovskii, *Phys. Rev. B* **81**, 064512 (2010).

[27] F.V. Kusmartsev, *Phys. Rev. Lett.* **76**, 1880 (1996).

[28] H. Yano, A. Handa, H. Nakagawa, K. Obara, O. Ishikawa, T. Hata, and M. Nakagawa, *J. Low Temp. Phys.* **138**, 561 (2005).

[29] D. Charamboulous, P.C. Hendry, L. Skrbek, P.V.E. McClintock, and W.F. Vinen, *CP850, Low Temperature Physics: 24th International Conference on Low Temperature Physics*, ed. Y. Takano, S.P. Hershfield, S.O. Hill, P.J. Hirschfeld, and A.M. Goldman, 205 (2006).

[30] E. Kozik and B. Svistunov, *Phys. Rev. B* **77**, 060502(R) (2008).